

UC Berkeley

UC Berkeley Previously Published Works

Title

Control of clustering behavior in anionic cerium(iii) corrole complexes: from oligomers to monomers

Permalink

<https://escholarship.org/uc/item/3191z4dk>

Journal

Dalton Transactions, 45(46)

ISSN

1477-9226

Authors

Armstrong, Keith C
Hohloch, Stephan
Lohrey, Trevor D
[et al.](#)

Publication Date

2016-11-22

DOI

10.1039/c6dt03884k

Peer reviewed



Published in final edited form as:

Dalton Trans. 2016 November 22; 45(46): 18653–18660. doi:10.1039/c6dt03884k.

Control of Clustering Behavior in Anionic Cerium(III) Corrole Complexes: From Oligomers to Monomers

B.Sc. Keith C. Armstrong^{a,†}, Dr. Stephan Hohloch^{a,†}, B.Sc. Trevor D. Lohrey^a, Dr. Ryan A. Zarkesh^b, Prof. Dr. John Arnold^a, and Prof. Dr. Mitchell R. Anstey^c

John Arnold: Arnold@berkeley.edu; Mitchell R. Anstey: mitch.anstey@davidson.edu

^aDepartment of Chemistry, University of California, Berkeley, 530 Latimer Hall, University of California, Berkeley, CA, 94720

^bSandia National Laboratories, 7011 East Avenue, Livermore, CA, 94550

^cDepartment of Chemistry, Davidson College, P.O. Box 7120, Davidson College, Davidson, NC, 28035

Abstract

The first synthesis of anion capped cerium corrole complexes is reported. Unusual clustering of the lanthanide corrole units has been found and the degree of aggregation can be controlled by the choice of the capping ligand. A polymeric structure **1a**, with the general formula [Cor-Ce(THF)-Cp-Na]_n (Cor = 5,15-bis(2,4,6-trimethylphenyl)-10-(4-methoxyphenyl)-corrole, THF = tetrahydrofuran), is formed using sodium cyclopentadienide (NaCp) and a dimeric structure **2a**, with the general formula [Cor-Ce-Tp]₂, is formed when potassium tris(pyrazolyl)borate (KTP) is used. Encapsulation of the counter-cation leads to the isolation of the monomeric structures **1b** and **2b**, with the general formulas [AM(2.2.2.-Cryptand)][Cor-Cp-X] (AM = Na or K, X = Cp or Tp). The structural and spectroscopic properties of the complexes have been investigated.

Introduction

Macrocyclic corrole chemistry has been a fast-developing area of modern inorganic and organometallic chemistry within the last few decades.¹ These tribasic, redox-active, strongly σ -donating ligands have been widely used to stabilize metals in various oxidation states.² In addition to their higher charge, these macrocycles distinguish themselves from porphyrins by their smaller core size. This constraint forces large metal ions out of the plane of the macrocycle,³ resulting in rigid steric protection on one side of the complex.^{1e,1i} The shielding of one side gives rise to several possibilities for fine-tuning reactivity and structure and thus has shown great promise, resulting in a wide variety of applications of these ligands, including catalysis, photochemical sensing, biomedical sensing and alternative energy applications.⁴

Correspondence to: John Arnold, Arnold@berkeley.edu; Mitchell R. Anstey, mitch.anstey@davidson.edu.

[†]Both these authors contributed equally to this work.

Electronic Supplementary Information (ESI) contains UV/Vis spectra, crystallographic table and monomeric views of **1a** and **2a**.

Lanthanides, on the other hand, have been used to great effect in single molecule magnets (SMM)⁵ and for biological imaging due to their low toxicity and unique electronic properties.⁶ With respect to the latter, strongly absorbing ligand scaffolds, e.g. conjugated macrocycles, are of great interest in lanthanide chemistry.^{6c, 7} To that end, there has been extensive work in the preparation and characterization of lanthanide porphyrin and phthalocyanine complexes ongoing since the 1970s.^{7b, 9–11} Considering the interest in tetrapyrroles and corroles being a member of this ligand family, it is remarkable that *f*-element corrole chemistry is still considerably underdeveloped.^{12,13}

To expand the diversity of lanthanide corrole coordination chemistry, we focused on the design of cerium corroles with anionic capping ligands. This approach was initially intended to offer additional coordination modes and improve structural stability but was met with unexpected clustering behaviour, including a 1D coordination polymer (**1a**). Comparing the oligomeric structures to their monomeric congeners, we found the Ce-corrole interaction to be strongly influenced by the encapsulation of the alkali metal: This change affected not only structural parameters but also spectroscopic properties. To compare the size effects of the lanthanide ion on the structural properties of the complexes, we also synthesized the monomeric lutetium analogue of one of the complexes.

Results and Discussion

Two different capping ligands, the cyclopentadienide anion (Cp, in **1**) and the tris(pyrazolyl)borate anion (Tp, in **2**), were employed. The corresponding complexes **1a** and **2a** were both synthesized following a one-pot, two-step procedure. To begin, the free base corrole was mixed with Ln(HMDS)₃ (Ln = Ce or Lu, HMDS = hexamethyldisilazide) in THF and stirred overnight as reported previously^{12a}. Subsequently, the crude material was used to access anionic complexes **1a** and **2a** by either addition of NaCp or KTp, respectively (Scheme 1).

Crystallization from a THF/hexane solution stored at –35 °C afforded complexes **1a** and **2a** as red/purple microcrystals in fair yields (55 – 75 %). The absence of diagnostic protonated corrole N-H stretches at 3200 cm⁻¹ provided the first indication of successful metalation. The purity of complexes **1a** and **2a** was corroborated by elemental analysis. While crystalline **1a** and **2a** could be handled under ambient conditions for several hours without visible decomposition, they decomposed quickly upon dissolution in the presence air and moisture. Inside a glove box however, the complexes were stable in solution for weeks. Complex **1a** crystallizes in the tetragonal space group *I*4₁/*a* with 16 formula units in the unit cell. In the solid state, **1a** forms a one-dimensional infinite helix structure. (compare Figure 1). The dihedral angle between two Ce(corrole) units (measured along the Na-Ce axis) is 86.3(1)°, corresponding to four molecular units per cycle and *S*₄-symmetry. The top view of **1a** shows the helix with an eight atom pitch (consistent with 4 molecular units per cycle). Purple lines thereby indicate Na-Cor-Ce units, while the green lines indicate Na1-Cp-Ce1 units. (Figure 2, top) The cerium atom is six-coordinate with the corrole ligand occupying four coordination sites, the Cp ligand one and the THF ligand one. The Ce-Cp distance is 2.599(1) Å with the Cp ligand slightly tilted showing a Cp_{cent} – Ce1 – N_{4plane} angle of 151.1°. We believe that this tilting of the Cp ligand results from the coordination of the THF

molecule to the cerium center. The cerium atom is dramatically shifted out of the N₄ plane of the corrole ring by 1.524(1) Å with an average N-Ce distance of 2.441(1) Å.

To the best of our knowledge, this is the largest out of plane distance reported for either a mononuclear heavy element corrole or porphyrin complex. (also compare SI, Table S3, S4 and S5 and Figure S7)^{8, 9-11, 12b} The Ce1-Na1 distance **1a** is 3.186(1) Å and the Ce1-Ce1 distance is 7.983(1) Å.

Crystals of **2a** were grown by slow diffusion of hexanes into a concentrated toluene solution. The complex crystallized in the triclinic space group P-1 with one molecule per unit cell. Surprisingly, **2a** also did not crystallize as a monomer but rather as a dimer (Figure 3). The asymmetric unit only displayed half of the molecule with an inversion center between the two potassium atoms. The K1-Ce1 metal distance was found to be 3.625(1) Å. The cerium atoms are separated by 12.065(1) Å, which is much further apart than those of **1a** (7.983(1) Å) and rule out any communication between the two metal centers. The cerium atom is sandwiched between the Tp and the corrole ligands with a Tp-Ce1-Cor angle of 176.1(1)° and devoid of coordinated solvent molecules. The resulting hepta-coordinate cerium atom of **2a** was also found to be far out of the plane of the macrocycle at a distance of 1.506(1) Å. (compare SI, Table S2, S3, S4 and S5)^{9-11, 12} The average distance of Ce1 to the nitrogen donors of the corrole is 2.548(1) Å. Looking from the other side, the distance from Ce1 to the Tp N₃ centroid is 1.914(1) Å, and the average distance from Ce1 to each Tp nitrogen is 2.617(1) Å. A summary of all structural data can be found in the SI in Tables S1 and S2.

Since the use of both the Cp ligand and the Tp ligand resulted in the formation of unexpected polymeric and dimeric structures, we then focused our interest on strategies to obtain the monomeric building blocks of **1a** and **2a**, respectively. We sought for the use of encapsulating molecules to strip out the alkali metals, since they form the bridging units in **1a** and **2a**. To ensure strong encapsulation of the alkali metals, 2.2.2.-cryptand was used as a sequestration agent. Addition of one equivalent of 2.2.2.-cryptand to reaction mixtures of **1a** and **2a** resulted in the clean formation of the desired monomeric compounds **1b** and **2b**. The purity and identity of the complexes were also supported by mass spectrometry, elemental analysis and X-ray analysis. As with compounds **1a** and **2a**, **1b** and **2b** were found to be moderately air stable as solids but decomposed rapidly in solution under air. Encapsulation of the alkali metals inhibited the formation of the solid state polymeric structure of **1a** and instead resulted in the formation of a single molecular species **1b**.

Crystals of **1b** were grown by slow evaporation of a concentrated DME/toluene solution. **1b** was found to crystallize in the triclinic space group P-1. Although Figure 4 suggests a κ^2 -bound DME ligand, inspection of the bonding situation reveals that one oxygen atom is closer bound to the cerium center (Ce1-O200 2.713(5) Å compared to Ce1-O201 2.820(5) Å, respectively), suggesting rather a κ^1 situation. The cerium atom is approximately 0.027 Å closer to the plane of the corrole ligand compared to the polymeric complex **1a**. Concurrently, the Cp ligand is 0.08 Å further away from the cerium center. This was unexpected, as the decoordination of the Cp to the sodium atom would increase the electron density on the Cp ligand, forcing it to move closer to the cerium ion. However, packing effects as well as steric repulsion from the DME ligand seem a larger factor and causes the

Cp ligand to move further away from the cerium center. This conclusion is supported by the fact that the $\text{Cp}_{\text{cent}}-\text{Ce1}-\text{N}_{4\text{plane}}$ angle was found to be slightly more tilted as compared to **1a** ($146.6(1)^\circ$ vs $151.9(1)^\circ$ respectively).

Crystals of **2b** were grown from a slow diffusion of hexane into a concentrated toluene solution. The complex crystallized in the orthorhombic space group *Pbca* with eight molecules in the unit cell. Similar as for **1a**, the formation of the dimeric structure **2a** was inhibited by encapsulation of the potassium ion and resulted in a well-defined monomeric species **2b**.

Comparing the structural parameters of **2a** with **2b**, the most recognizable change is the out of plane coordination of the cerium center. As expected, relocating the potassium ion to the outer sphere of the complex allows the cerium atom to move closer to the N_4 plane by 0.067\AA , reducing the N_4 plane-metal distance from $1.506(1)\text{\AA}$ in **2a** to $1.439(1)\text{\AA}$ in **2b**. The average Ce-N distance was found to be 2.424\AA . The tighter cerium corrole coordination led to an elongation of the Ce1-Tp centroid distance by 0.07\AA , and a new Ce1-Tp centroid distance of $1.986(1)\text{\AA}$ and an average Ce1- N_{Tp} distance of 2.665\AA . This elongation is likely due to steric effects between the corrole and the Tp ligand rather than an electronic effect. Besides these differences, the structural parameters of **2b** were found to be essentially the same as those in **2a**, with a hepta-coordinated cerium atom, sandwiched in an almost linear arrangement ($\text{Cor}_{\text{centroid}}-\text{Ce1}-\text{Tp}_{\text{centroid}}$ $175.1(1)^\circ$) between the corrole and the Tp ligand. For further details, please see Tables S1 and S2 in the SI.

With structural characterization of **1a**, **1b**, **2a** and **2b** complete, our studies turned toward probing the influence of lanthanide ion size on structural diversity. Therefore, these same syntheses were attempted using analogous tris(bis(trimethylsilyl)amino) lutetium(III) ($\text{Lu}(\text{HMDS})_3$) starting materials. Unfortunately, the same procedures led only to the isolation of crystalline material for the lutetium analogue of **1b**, namely **3b**. The low yield ($<1\%$) prevented additional characterization beyond X-ray structural analysis. Nonetheless, comparing the structure of **3b** to **1b** revealed substantial differences. (Compare Figure 6). X-Ray quality crystals of **3b** were grown from layering a THF solution of **3b** with hexane. Complex **3b** also crystallized in the triclinic space group P-1 with two toluene molecules within the lattice. In contrast to **1a** and **1b**, **3b** does not contain additional solvent molecules coordinated to the metal center. In **3b**, the lutetium center sits only $1.091(1)\text{\AA}$ above the corrole plane. Additionally, the distance from the Cp centroid to the lanthanide ion shrinks from $\sim 2.6\text{\AA}$ in **1a** and **1b** to only $2.335(1)\text{\AA}$ in **3b**. Due to the much smaller ionic radius of Lu(III) compared to Ce(III), the steric congestion around the metal center in **3b** is greater and likely prevents the coordination of additional solvent. This steric crowding also results in more repulsion between the Cp ligand and the corrole, affording an almost parallel orientation of the corrole and the Cp ligand planes lutetium ion (compare Table S2).

UV/Vis spectroscopy

In addition to structural characterizations of all complexes, we investigated the UV/Vis spectra of the complexes **1** and **2** in THF (**3b** was not isolated in sufficient yield to be characterized by this method, as previously mentioned). We found the encapsulation of the

counter ion seems to have a larger impact on the electronic structure of such molecules than expected. Encapsulation of the alkali metals lead to a blue shift of the soret bands in all complexes. While going from **1a** to **1b** the difference is rather small (433 to 435 nm for **1a** and **1b** respectively); in the case of **2** the effects were already visible to the eye, as **2a** appears to be more bluish in colour compared to **2b**. The soret bands for **2a** can be found at 434 nm while the maximum for **2b** lies at 443 nm. It is not clear at this time what change is causing the blue shift, but we speculate that structural changes of **1a** and **2a** occur upon encapsulation of the alkali metal possibly akin to the differences noted in the corresponding X-ray crystal structures. The absorption maxima of these complexes could be influenced by the out-of-plane coordination of the lanthanide ion as the Ce-Cor_{centroid} distance of **2a** to **2b** is bigger (0.067 Å) than **1a** to **1b** (0.027 Å). However, especially in the case from **1a** to **1b**, the presence of a THF ligand in place of a DME ligand could affect the absorption maxima as well. The solution-phase molecular structure has to be more closely investigated before any definitive statement on this matter can be made.

Conclusions

In conclusion, the first examples of cerium and lutetium corrole complexes have been isolated as well as the first examples of lanthanide corrole complexes with anionic capping ligands. In view of the fact that the reported complexes can be synthesized in well-defined and reproducible structural conformations, this work should have a significant impact on the future of heavy element corrole chemistry, inspiring researchers to investigate new corrole complexes for magnetic, photophysical, and catalytic studies.

Experimental section

Methods and Materials

All manipulations were performed under inert gas using nitrogen-atmosphere glovebox techniques. Solvents were degassed by sparging with nitrogen and dried by passing through a column of activated alumina. UV-visible spectra were determined with a Varian Cary 50 UV-vis spectrophotometer using a 10 mm quartz cell in THF. Mass spectral data (ESI-MS/ion trap, negative mode) were obtained at the University of California, Berkeley Microanalytical Facility. X-ray crystal diffraction data was collected at the University of California, Berkeley CHEXRAY facility, at the Lawrence Berkeley National Laboratory Advanced Light Source, and at Sandia National Laboratories. Melting points were determined using sealed capillaries prepared under nitrogen and are uncorrected. Tris(bis(trimethylsilyl)amino)cerium(III) (Ce(HMDS)₃; CeN₃*), Tris(bis(trimethylsilyl)amino)lutetium(III) (Lu(HMDS)₃; LuN₃*)¹⁴ and 5,15-bis(2,4,6-trimethylphenyl)-10-(4-methoxyphenyl)-corrole (Mes₂Ani-corrole)^{13b} were prepared according to previously reported procedures. Cyclopentadienylsodium, potassium tris(pyrazolyl)borate and 2.2.2-cryptand were obtained from Aldrich.

General procedures

In the glovebox, a solution of Ln(HMDS)₃ (Ln = Ce or Lu, HMDS = hexamethyldisilazide, 1 eq) in THF (5 mL) was added dropwise to a solution of Mes₂Ani-corrole (1 eq) in THF (5

mL) in a vial at ca. -35°C . The resulting solution was allowed to warm to room temperature and stirred overnight, after which time the colour had changed from dark purple to dark green. The solvent was then removed *in vacuo* to give an oily green residue and triturated with hexanes (3×2 mL). The residue was thoroughly dried and redissolved in THF (5 mL). A solution of the capping ligand (1.05 eq) in THF (5 ml) was then added to this solution at room temperature in one portion, followed by 2.2.2-cryptand (1.05 eq) if necessary. The resulting solution was allowed to stir overnight. Bulk material was obtained by removing the solvent *in vacuo* and furthering triturating the residue with hexanes (3×2 mL) to give an oily residue. Microcrystalline dark green material was obtained from recrystallization of the bulk material from THF layered by hexane.

Poly(sodium cyclopentadienyl tetrahydrofuran cerium(III) 5,15-bis(2,4,6-trimethylphenyl)-10-(4-methoxyphenyl)-corrole) (1a)—From $\text{Ce}(\text{HMDS})_3$ (43.1 mg, 0.068 mmol) and NaCp (6.3 mg, 0.071 mmol) Dark green powder Yield : 39 mg, 0.0414 mmol, 61% yield. Single crystals suitable for X-ray diffraction were grown by storing a concentrated THF/hexane mixture at -35°C for several days. Elemental analysis: Calcd for $\text{C}_{53}\text{H}_{50}\text{N}_4\text{O}_2\text{Ce}_1\text{Na}_1$ C 67.86%, H 5.37%, N 5.97%; found: C 67.09%, H 7.11%, N 7.80%. UV-vis (nm): 434 (47100), 630 (16200). Mp: decomp over 300°C .

(2.2.2-Cryptand) sodium cyclopentadienyl cerium(III) 5,15-bis(2,4,6-trimethylphenyl)-10-(4-methoxyphenyl)-corrole (1b)—From $\text{Ce}(\text{HMDS})_3$ (43.1 mg, 0.068 mmol), NaCp (6.3 mg, 0.071 mmol) and 2.2.2-cryptand (26.6 mg, 0.071 mmol). In order to obtain pure material, the complex was additionally recrystallized from DME/Hexane. Yield: 51 mg, 0.038 mmol, 56%. To obtain x-ray quality material the compound was recrystallized by slow evaporation of a Toluene/DME (2:1) mixture. Elemental analysis: Calcd for $\text{C}_{71}\text{H}_{88}\text{N}_6\text{O}_9\text{Ce}_1\text{Na}_1$ 3.2 DME: C 62.09%, H 7.46%, N 5.18%; found: C 61.26 %, H 7.01%, N 6.04%. UV-vis (nm): 442 (36200), 630 (14200). Mp: decomp over 300°C .

Trispyrazolylborato cerium(III) 5,15-bis(2,4,6-trimethylphenyl)-10-(4-methoxyphenyl)-corrole potassium dimer (2a)—From $\text{Ce}(\text{HMDS})_3$ (43.1 mg, 0.068 mmol) and KTp (17.8 mg, 0.071 mmol). Yield: 51 mg, 0.026 mmol, 75%. Single crystals suitable for X-ray diffraction were grown by vapor diffusion of hexanes into a concentrated solution of toluene at room temperature. Elemental analysis: Calcd for $\text{C}_{106}\text{H}_{94}\text{N}_{20}\text{O}_2\text{B}_2\text{Ce}_2$: C 61.80%, H 4.60%, N 13.60%; found: C 61.60%, H 4.53%, N 13.48%. UV-vis (nm): 437 (98500), 625 (24100). ESI-MS from THF solution (–) Calcd: 990.3082 for $[\text{C}_{53}\text{H}_{47}\text{N}_{10}\text{B}_1\text{O}_1\text{Ce}_1]^{-}$, Observed: 990.3120. Mp: decomp over 300°C .

(2.2.2-Cryptand) potassium trispyrazolylborato cerium(III) 5,15-bis(2,4,6-trimethylphenyl)-10-(4-methoxyphenyl)-corrole (2b)—From $\text{Ce}(\text{HMDS})_3$ (43.1 mg, 0.068 mmol). KTp (17.8 mg, 0.071 mmol) and 2.2.2-cryptand (26.6 mg, 0.071 mmol). Yield: 53 mg, 0.037 mmol, 55%. Single crystals suitable for X-ray diffraction were grown by vapor diffusion of pentane into a concentrated solution of dichloromethane at room temperature. Elemental analysis: Calcd for $\text{C}_{71}\text{H}_{83}\text{N}_{12}\text{O}_7\text{B}_1\text{Ce}_1\text{K}_1$: C 60.63 %, H 5.95 % N 11.95 %; found: C 61.04%, H 6.25%, N 12.11%. UV-vis (nm): 444 (79500), 630 (20800)

ESI-MS (–) ESI-MS from THF solution (–) Calcd: 990.3082 for $[\text{C}_{53}\text{H}_{47}\text{N}_{10}\text{B}_1\text{O}_1\text{Ce}_1]^-$,
Observed: 990.3119. Mp: decomp over 300°C.

(2.2.2-Cryptand) sodium cyclopentadienyl lutetium(III) 5,15-bis(2,4,6-trimethylphenyl)-10-(4-methoxyphenyl)-corrole (3b)—From $\text{Lu}(\text{HMDS})_3$ (44.6 mg, 0.068 mmol), NaCp (6.3 mg, 0.071 mmol) and 2.2.2-cryptand (26.6 mg, 0.071 mmol). Only few crystals observed. No yield determined but less than 1%.

X-Ray crystallography

X-ray structural determinations were performed at CHEXRAY, University of California, Berkeley, on a Bruker APEX II Quazar diffractometer, at the Sandia National Laboratories on a SuperNova diffractometer (Oxford Diffraction) or at the Advanced Light Source (ALS) at the Lawrence Berkeley National Laboratories. The Bruker Quazar and the SuperNova are Kappa Geometry and are three-circle diffractometers that couples a charge-coupled device (CCD) detector with a sealed-tube source of monochromatized $\text{Mo K}\alpha$ radiation. The ALS is Kappa Geometry using a silicon monochromated beam with an energy of 16keV (= 0.7749 Å). Crystals of appropriate size were coated in Paratone-N oil and mounted on a Kaptan loop. The loop was transferred to the diffractometer, centered in the beam, and cooled by a nitrogen flow low-temperature apparatus that had been previously calibrated by a thermocouple placed at the same position as the crystal. The data were corrected for Lorentz and polarization effects; no correction for crystal decay was applied. An empirical absorption correction based on comparison of redundant and equivalent reflections was applied using SADABS. All software used for diffraction data processing and crystal-structure solution and refinement are contained in the APEX3 program suite (Bruker AXS, Madison, WI). Thermal parameters for all non-hydrogen atoms were refined anisotropically.¹⁵ CCDC numbers for the complexes **1a**, **1b**, **2a**, **2b** and **3b** can be found in Table S1. The CIF-Files can be downloaded free of charge from <https://summary.ccdc.cam.ac.uk/structure-summary-form>.

Supplementary Material

Refer to Web version on PubMed Central for supplementary material.

Acknowledgments

We thank the NSF (Grant CHE-1465188), the German Academic Exchange Service (DAAD), and Davidson College for financial support and for a postdoctoral fellowship. We also acknowledge the Advanced Light Source, which is supported by the Director, Office of Science, Office of Basic Energy Sciences, of the U.S. Department of Energy under Contract No. DE-AC02-05CH11231. Dr. Simon Teat from the ALS is also kindly acknowledged for help with measurements on the synchrotron. Furthermore, we also would like to thank the NIH (Grant S10-RR027172) for financial support of our X-Ray crystallographic facility. Mary E. Garner and Dr. Bernd M. Schmidt are kindly acknowledged for comments and helpful discussions.

Notes and references

1. a) Aviv-Harel I, Gross Z, *Coord. Chem. Rev.* 2010; 255:717–736. b) Simkhovich L, Galili N, Saltsman I, Goldberg I, Gross Z. *Inorg. Chem.* 2000; 39:2704–2705. [PubMed: 11232801] c) Luobeznova I, Simkhovich L, Goldberg I, Gross Z. *Eur. J. Inorg. Chem.* 2004:1724–1732. d) Thomas KE, Wasbotten IH, Ghosh A. *Inorg. Chem.* 2008; 47:10469–10478. [PubMed: 18928275]

- e) Aviv-Harel I, Gross Z. *Chem. Eur. J.* 2009; 15:8382–8394. [PubMed: 19630016] f) Palmer JH. *Struct. Bonding.* 2012; 142:49–90. g) Thomas KE, Alemayehu AB, Conradie J, Beavers CM, Ghosh A. *Acc. Chem. Res.* 2012; 45:1203–1214. [PubMed: 22444488] h) Buckley HL, Chomitz WA, Koszarna B, Tasior M, Gryko DT, Brothers PJ, Arnold J. *Chem. Commun.* 2012; 48:10766–10768. i) Aviv I, Gross Z. *Chem. Commun.* 2007; 20:1987–1999. j) Thomas KE, Alemayehu AB, Conradie J, Beavers CM, Ghosh A. *Acc. Chem. Res.* 2012; 45:1203–1214. [PubMed: 22444488] k) Ooi S, Tanaka T, Park KH, Kim D, Osuka A. *Angew. Chem Int. Ed.* 2016; 55:6561. l) Ooi S, Tanaka T, Osuka A. *Inorg. Chem.* 2016
2. a) Woormileela S, Sommer MG, Deibel N, Ehret F, Bauer M, Sarkar B, Kar S. *Angew. Chem. Int. Ed.* 2015; 54:13769–13774. b) Kumar A, Goldberg I, Botohansky M, Buchman Z, Gross Z. *J. Am. Chem. Soc.* 2010; 132:15233–15245. [PubMed: 20932015] c) Palmer JH, Day MW, Wilson AD, Henling LM, Gross Z, Gray HB. *J. Am. Chem. Soc.* 2008; 130:7786–7787. [PubMed: 18512923] d) Lai W, Cao R, Dong G, Shaik S, Yao J, Chen H. *J. Phys. Chem. Lett.* 2012; 3:2315–2319. [PubMed: 26292109] e) Rosa P, Buckley HL, Ward AL, Arnold J. *J. Porphyrins Phthalocyanines.* 2016; 19:150–153. f) Buckley HL, Rubin LK, Chrominski M, McNicholas BJ, Tsen KHY, Gryko DT, Arnold J. *Inorg. Chem.* 2014; 53:7941–7950. [PubMed: 25029670] g) Sinha W, Deibel N, Agarwala H, Garai A, Schweinfurth D, Purohit Cs, Lahiri GK, Sarkar B, Kar S. *Inorg. Chem.* 2014; 53:1417–1429. [PubMed: 24432714] h) Sinha W, Kumar M, Garai A, Purohit CS, Som T, Kar S. *Dalton Trans.* 2014; 43:12564–12573. [PubMed: 25005871] i) Sinha W, Sommer MG, Deibel N, Ehret F, Sarkar B. *Chem. Eur. J.* 2014; 15:15920–15932. [PubMed: 25280161] j) Vazquez-Lima H, Conradie J, Ghosh A. *Inorg. Chem.* 2016. k) Wasbotten IH, Wondigmagegn T, Ghosh A. *J. Am. Chem. Soc.* 2002; 124:8104–8116. [PubMed: 12095356] l) Wasbotten I, Ghosh A. *Inorg. Chem.* 2006; 45:4910–4913. [PubMed: 16780311]
3. a) Palmer JH, Durrell AC, Gross Z, Winkler JR, Gray HB. *J. Am. Chem. Soc.* 2010; 132:9230–9231. [PubMed: 20568752] b) Alemayehu AB, Ghosh A. *J. Porphyrins Phthalocyanines.* 2011; 15:106–110. c) Rabinovich E, Goldberg I, Gross Z. *Chem. Eur. J.* 2011; 17:12294–12301. [PubMed: 21972002] d) Thomas KE, Alemayehu AB, Conradie J, Beavers C, Ghosh A. *Inorg. Chem.* 2011; 50:12844–12851. [PubMed: 22111600] e) Schoefberger W, Lengwin F, Reith LM, List M, Knoer G. *Inorg. Chem. Commun.* 2010; 13:1187–1190. f) Reith LM, Himmelsbach M, Schoefberger W, Knoer G. *J. Photochem. Photobiol., A.* 2011; 218:247–253. g) Buckley HL, Arnold J. *Dalton Trans.* 2015; 44:30–36. [PubMed: 25321078]
4. a) Palmer, JH. *Structure and Bonding*, Vol 142. Vol. 49. Berlin: Springer; 2011. b) Aviv-Harel I, Gross Z. *Coord. Chem. Rev.* 2010; 7:1. c) Gross Z. *J. Biol. Inorg. Chem.* 2001; 6:733. [PubMed: 11681707]
5. a) Ishikawa N, Sugita M, Ishikawa T, Koshihara S-Y, Kaizu Y. *J. Am. Chem. Soc.* 2003; 125:8694–8695. [PubMed: 12862442] b) Woodruff DN, Winpenny R, Layfield RA. *Chem. Rev.* 2013. c) Luzon J, Sessoli R. *Dalton Trans.* 2012; 41:13556–13567. [PubMed: 22936346] d) Sorace L, Benelli C, Gatteschi D. *Chem. Soc. Rev.* 2011; 40:3092. [PubMed: 21390351]
6. a) Bünzli J-CG. *Acc. Chem. Res.* 2006; 39:53–61. [PubMed: 16411740] b) Bünzli J-CG. *Chem. Rev.* 2010; 110:2729–2755. [PubMed: 20151630] c) Parker D, Dickens R, Puschmann H. *Chem. Rev.* 2002; 102:1977–2010. [PubMed: 12059260] d) Richardson FS. *Chem. Rev.* 1982; 82:541–552. e) Moore EG, Samuel APS, Raymond KN. *Acc. Chem. Res.* 2009; 42:542–552. [PubMed: 19323456] f) Das GK, Tan TTT. *J. Phys. Chem. C.* 2008; 112:11211–11217.
7. a) Alexander V. *Chem. Rev.* 1995; 95:273–342. b) Horrocks WD Jr, Wong CP. *J. Am. Chem. Soc.* 1976; 98:7157–7162. [PubMed: 977867] c) Khalil GE, Thompson EK, Gouterman M, Callis JB, Dalton LR, Turro NJ, Jockusch S. *Chem. Phys. Lett.* 2007; 435:45–49.
8. The only complexes showing a larger out-of-plane coordination is the triple-decker di-europium-diphtalocyanine corrole complex (1.79(1) Å) reported by Kadish and co-workers. 13b However in this complex, the central corrole ring is not puckered towards the europium center but is instead planar, probably due to steric repulsion between the phthalocyanide and the corrole. The large distance therefore could indicate a coulombic rather than a covalent interaction between the corrole and the europium ion.
9. a) Jiang J, Ng DKP. *Acc. Chem. Res.* 2009; 42:79–88. [PubMed: 18767871] b) Zhu X, Wong W-K, Wong W-Y, Yang X. *Eur. J. Inorg. Chem.* 2011; 4651–4674. c) Moussavi M, De Cian A, Fischer J, Weiss R. *Inorg. Chem.* 1986; 25:2107–2108. d) Buchler JW, Kapellmann H-G, Knoff M, Lay K-L, Pfeifer S. *Z. Naturforsch., B.* 1983; 38:1339–1345. e) George S, Lipstman S, Goldberg I. *Cryst.*

- Growth Des. 2006; 6:2651–2654.f) Ishikawa N, Kaizu Y. *Coord. Chem. Rev.* 2002; 226:93–101.g) Gross T, Chevalier F, Lindsey JS. *Inorg. Chem.* 2001; 40:4762–4774. [PubMed: 11511227]
10. Selected references for early Ln porphyrin complexes (La-Nd): Ikeda M, Takuchi M, Sugasaki A, Robertson A, Imada T, Shinkai S. 2000; 12:321–345. Bian Y, Jiang J- Tao Y, Choi MTM, Li R, Ng ACH, Zhu P, Pan N, Sun X, Arnold DP, Zhou Z-Y, Li H-W, Mak TCW, Ng DKP. *J. Am. Chem. Soc.* 2003; 125:12257–12267. [PubMed: 14519011] Bian Y, Wang D, Wang R, Weng L, Dou J, Zhao D, Ng DKP, Jiang J. *New J. Chem.* 2003; 27:844–849. Zhang Y, Cao W, Wang K, Jiang J. *Dalton Trans.* 2014; 43:9152–9157. [PubMed: 24809442] He H, Wong W-K, Guo J, Li K-F, Wong W-Y, Cheah K-W. *Aust. J. Chem.* 2004; 57:803–810. Buchler JW, de Cian A, Fischer J, Kihn-Botulinski M, Paulus H, Weiss R. *J. Am. Chem. Soc.* 1986; 108:3652–3659. He H, Wong W-K, Guo J, Li K-F, Wong W-Y, Lit W-K, Cheah K-W. *Inorg. Chim. Acta.* 2004; 357:4379–4388. Foley TJ, Harrison BS, Knefely AS, Abboud KA, Reynolds JR, Schanze KS, Boncella JM. *Inorg. Chem.* 2003; 42:5023–5032. [PubMed: 12895128] Chabach D, Lachkar M, De Cian A, Fischer J, Weiss R. *New J. Chem.* 1992; 16:431. Lachkar M, de Cian A, Fischer J, Weiss R. *New J. Chem.* 1988; 12:729. Buchler JW, Scharbert B, Englert U, Strahle J. *Chem. Ber.* 1988; 121:2077–2082. Chabach D, De Cian A, Fischer J, Weiss R, Bibout BEM. *Angew. Chem. Int. Ed.* 1996; 35:898–899. Tahiri M, Chabach D, Malouli-Bibout ME, De Cian A, Fischer J, Weiss R. *Ann. Chim.* 1995; 20:81. Jiang J, Bian Y, Liu W, Choi MTM, Kobayashi N, Li H-W, Yang Q, Mak TCW, Ng DKP. *Chem. Eur. J.* 2001; 7:5059–5069. [PubMed: 11775679] Buchler JW, De Cian A, Fischer J, Hammerschmitt P, Löffler J, Scharbert B, Weiss R. *Chem. Ber.* 1989; 122:2219–2228. Chabach D, Tahiri M, de Cian A, Fischer J, Weiss R, Bibout MEM. *J. Am. Chem. Soc.* 1995; 117:8548–8556.
11. Selected references for lutetium porphyrin complexes: Zhu P, Zhang X, Wang H, Bian Y, Jiang J. *Inorg. Chem.* 2012; 51:5651–5659. [PubMed: 22554027] Sun R, Wu X, Zhang X. *Inorg. Chim. Acta.* 2012; 384:204–209. Lachkar M, Tabard A, Brandes S, Guillard R, De Cian A, Fischer J, Weiss R. *Inorg. Chem.* 1997; 36:4141–4146. Jiang J, Bian Y, Furuya F, Liu W, Choi MTM, Kobayashi N, Li H-W, Yang Q, Mak TCW, Ng DKP. *Chem. Eur. J.* 2001; 7:5059–5069. [PubMed: 11775679] Schavarién CJ, Orpen AG. *Inorg. Chem.* 1991; 30:4968–4978.
12. a) Buckley HL, Anstey MR, Gryko DT, Arnold J. *Chem. Commun.* 2013; 49:3104–3106. b) Lu G, Yan S, Shi M, Yu W, Li J, Zhu W, Ou Z, Kadish KM. *Chem. Commun.* 2015; 51:2411–2413.
13. Ward AL, Buckley HL, Lukens WW, Arnold J. *J. Am. Chem. Soc.* 2013; 135:13965–13971. [PubMed: 24004416]
14. Bradley DC, Ghotra JS, Hart FAJ. *J. Chem. Soc., Dalton Trans.* 1973; 10:1021–1023.
15. a) SMART: Area Detector Software Package. Madison WI: Bruker Analytical X-ray Systems Inc.; 2003. b) SADABS: Bruker-Nonius Area Detector Scaling and Absorption, V2.05. Madison, WI: Bruker Analytical X-ray Systems Inc.; 2003. c) Sheldrick GM. *Acta Crystallogr., A.* 2008; 64:112. [PubMed: 18156677] d) Farrugia LJ. *Appl. Crystallogr.* 1997; 30:565. e) van der Sluis P, Spek AL. *Acta Crystallogr., A.* 1990; 46:194.

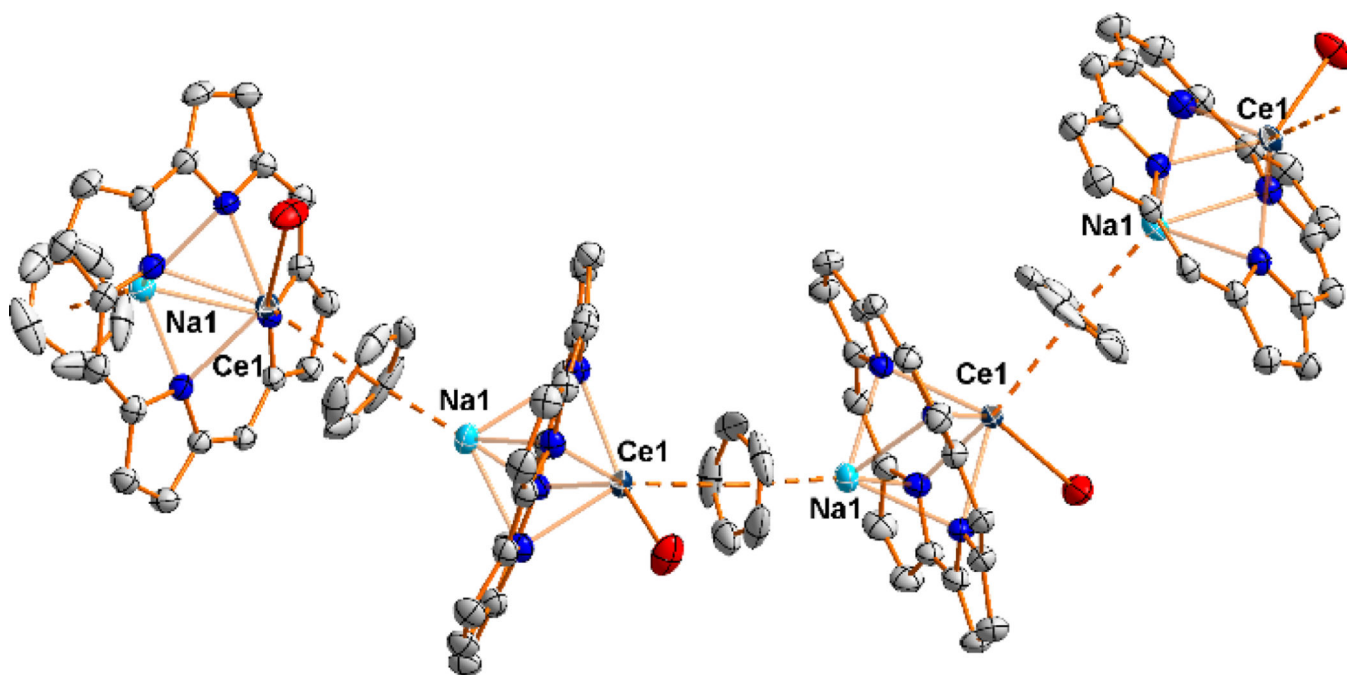


Figure 1.

Molecular structure of polymeric **1a** in the solid state. Thermal ellipsoids are shown at a probability level of 50%. Hydrogen atoms, as well as the carbon atoms of the THF ligand and the mesityl and anisole residues on the corrole ligand have been omitted for clarity. Selected bond lengths (Å): Ce1 – O200, 2.558(3), Ce1 – N_{4plane} 1.524(1), Na1 – N_{4plane} 1.660(1), Cp_{cent} – Ce1 2.599(1), Cp_{cent} – Na1 2.389(1), Na1 – Ce1 3.186(1). Selected bond angles (°): N_{4plane} – Ce1 – Cp_{cent} 151.1(1).

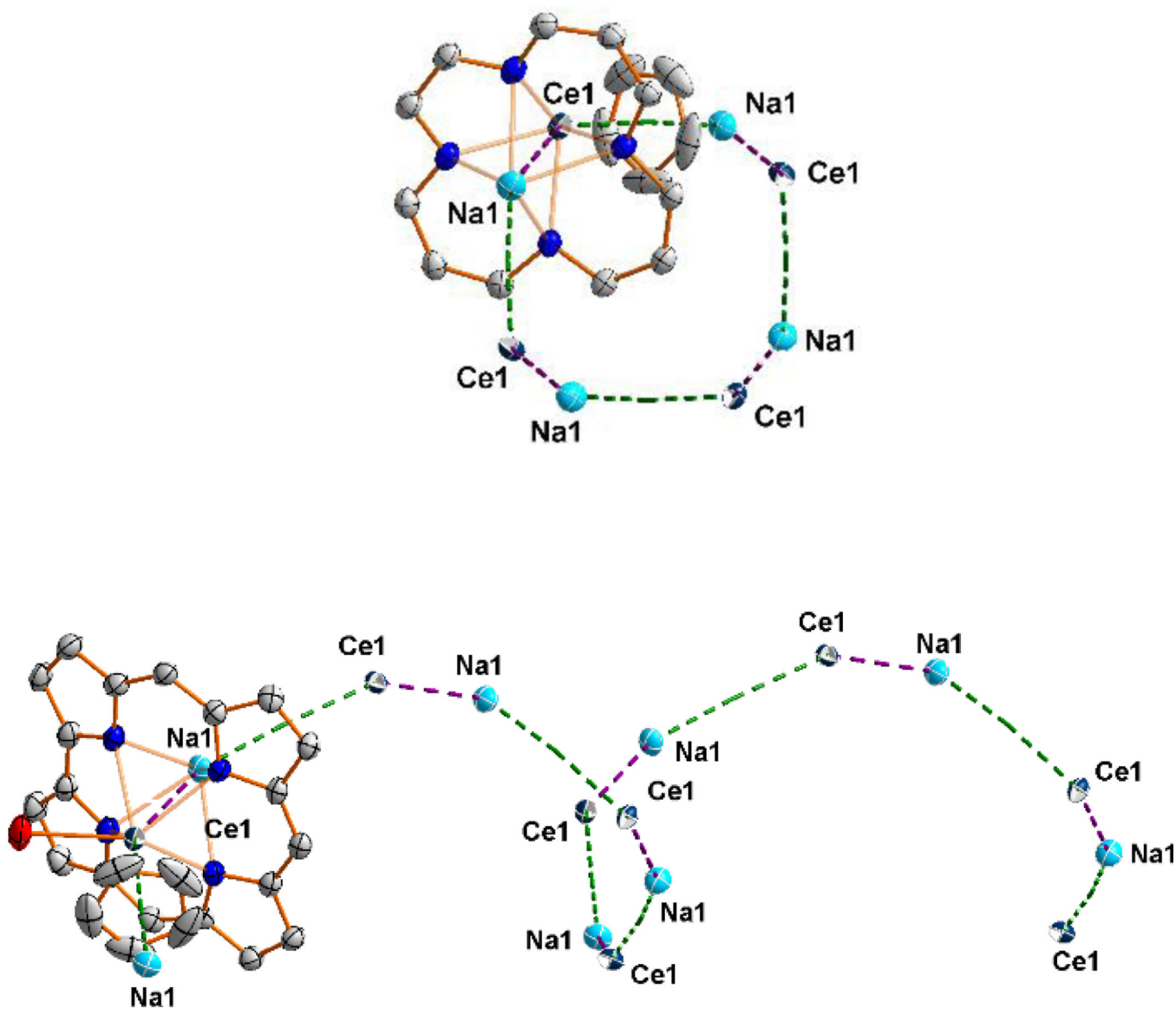


Figure 2.

View along the screw axis in **1a** (top). Side view of the helix (bottom). A monomeric view of the CpCe(corrole) units can be found in the SI, Figure S5. For further clarification, the Na1-Ce1 distances (going through the $N_{4\text{plane}}$ of the corrole) are coloured in violet, while the Ce1-Cp_{cent} and the Na1-Cp_{cent} are marked in orange. Thermal ellipsoids are shown at a probability level of 50%. Hydrogen atoms, as well as the carbon atoms of the THF ligand and the mesityl and anisole residues on the corrole ligand have been omitted for clarity.

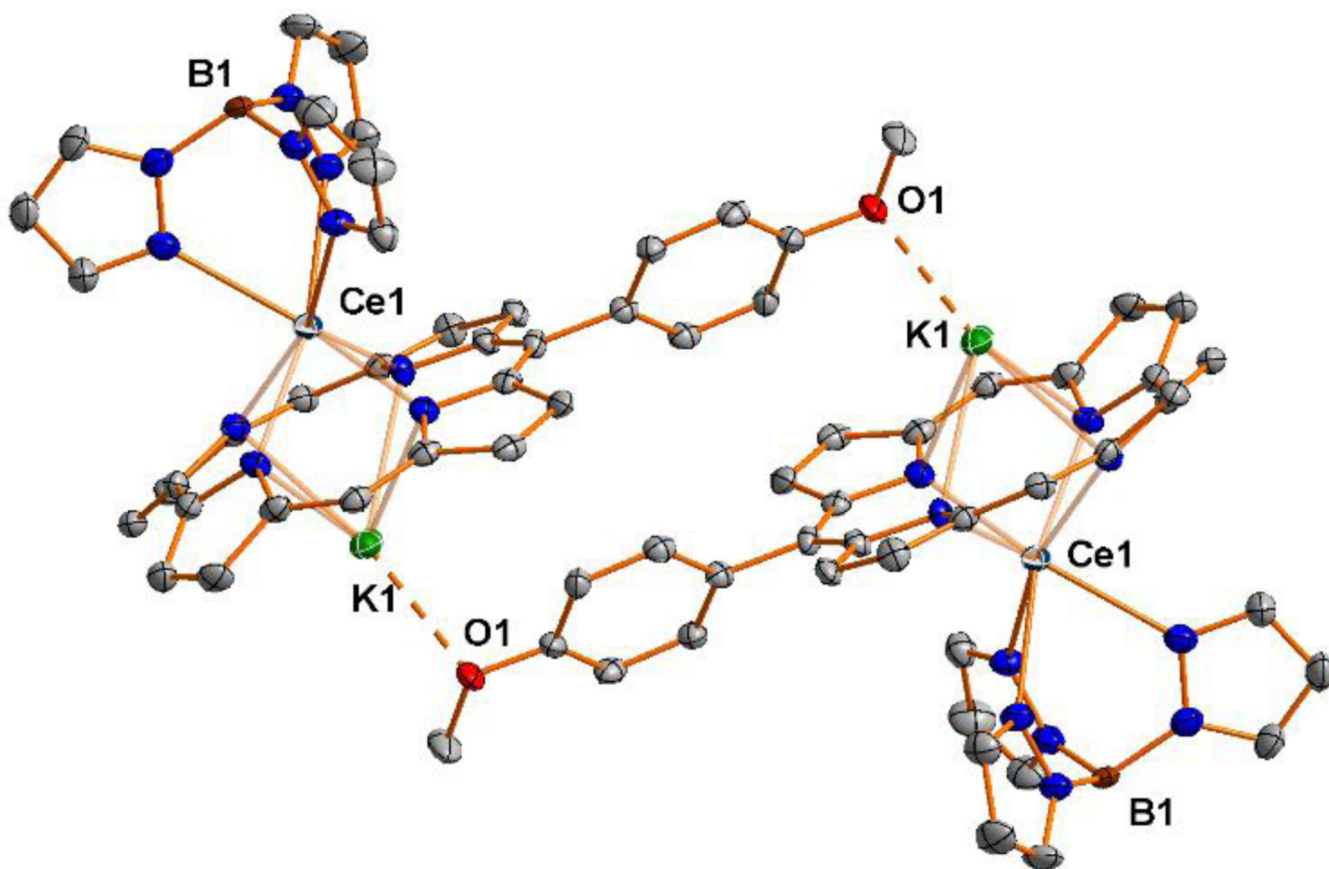


Figure 3. Molecular structure of dimeric **2a** in the solid state. A monomeric view of the TpCe(corrole) units can be found in the SI, Figure S6. Thermal ellipsoids are shown at a probability level of 50%. Hydrogen atoms, as well as the carbon atoms of the THF ligand and the mesityl residues on the corrole ligand have been omitted for clarity. Selected bond lengths (Å): Ce1 – N_{4plane} 1.506(1), K1 – N_{4plane} 2.116(1), Tp_{cent} – Ce1 1.914(1), K1 – Ce1 3.625(1), O1 – K1 2.643(3). Selected bond angles (°): N_{4plane} – Ce1 – Tp_{cent} 176.7(1).

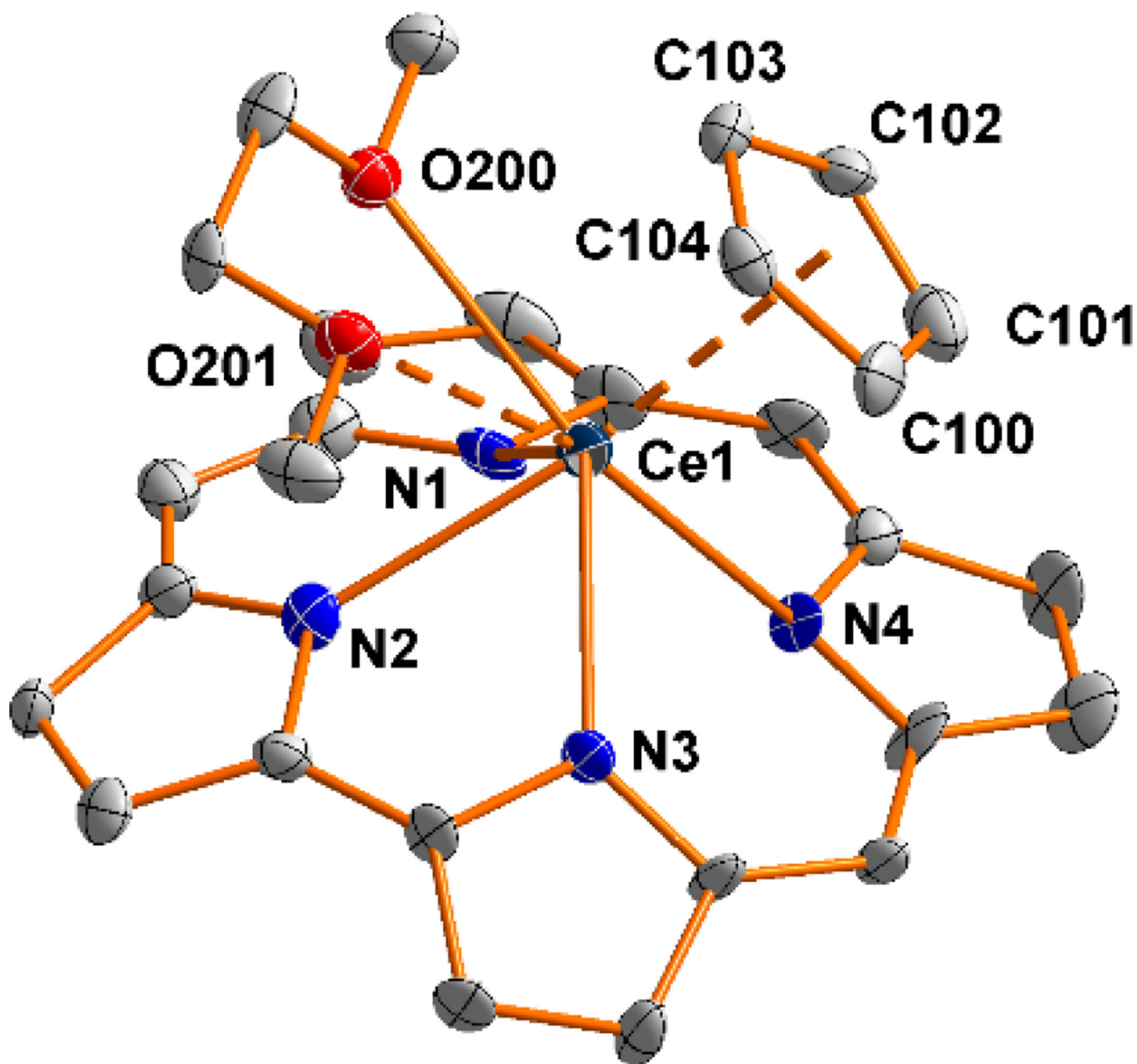


Figure 4. Molecular structure of **1b** in the solid state. Thermal ellipsoids are shown at a probability level of 50%. Hydrogen atoms, the cryptand sodium, the mesityl and the anisole residues on the corrole ligand have been omitted for clarity. Selected bond lengths (Å): Ce1 – O200, 2.713(5), Ce1 – O201 (2.820(5), Ce1 – N_{4plane} 1.497(1), Cp_{cent} – Ce1 2.666(1). Selected bond angles (°): N_{4plane} – Ce1 – Cp_{cent} 146.6(1).

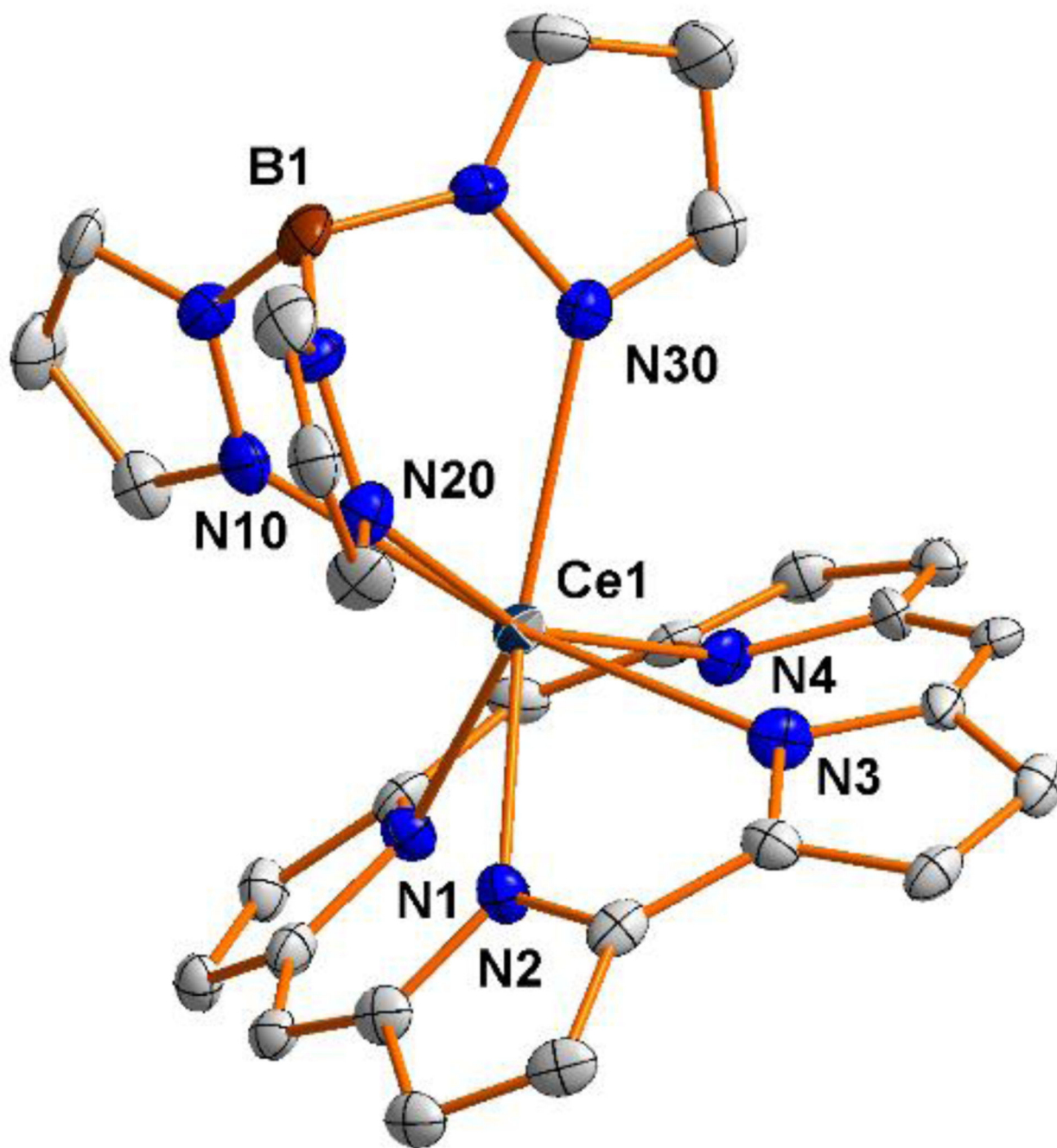


Figure 5. Molecular structure of **2b** in the solid state. Thermal ellipsoids are shown at a probability level of 50%. Hydrogen atoms, the cryptand potassium, the mesityl and the anisole residues on the corrole ligand have been omitted for clarity. Selected bond lengths (Å): Ce1 – N_{4plane} 1.439(1), K1 – Ce1 1.986(1). Selected bond angles (°): N_{4plane} – Ce1 – K1 175.1(1).

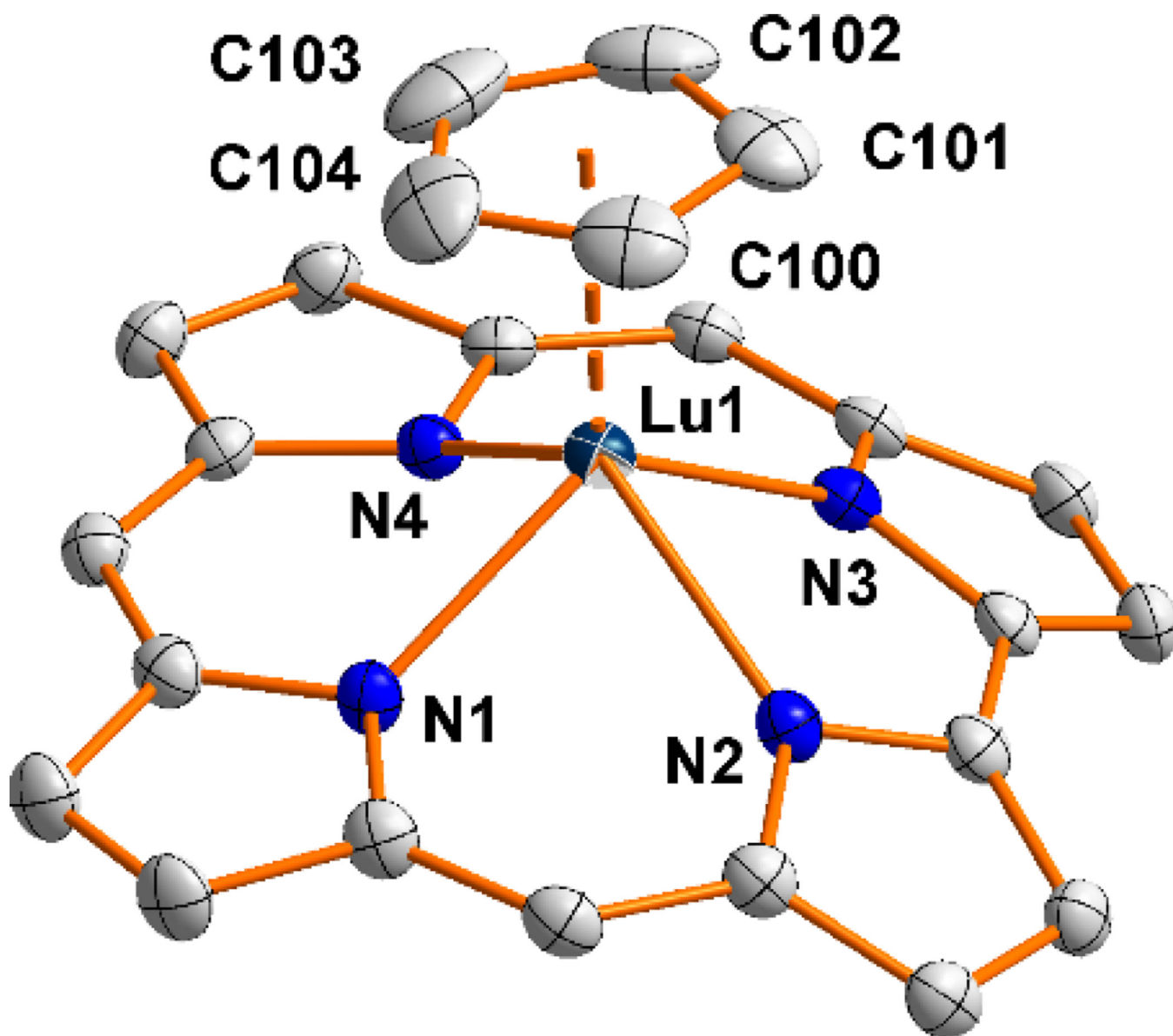


Figure 6. Molecular structure of **3b** in the solid state. Thermal ellipsoids are shown at a probability level of 50%. Hydrogen atoms, the cryptated sodium, the mesityl and the anisole residues on the corrole ligand have been omitted for clarity. Selected bond lengths (Å): Lu1 – N_{4plane} 1.091(1), Cp_{cent} – Ce1 2.335(1). Selected bond angles (°): N_{4plane} – Ce1 – Cp_{cent} 177.4(1).

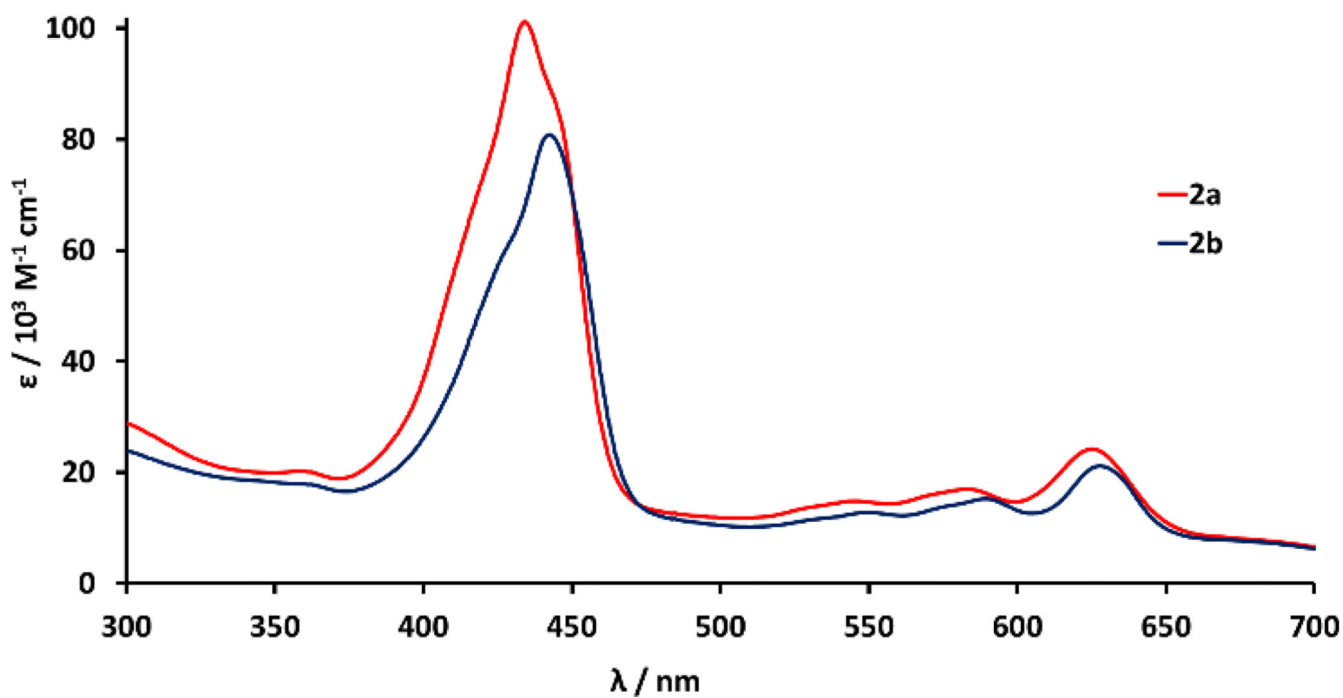
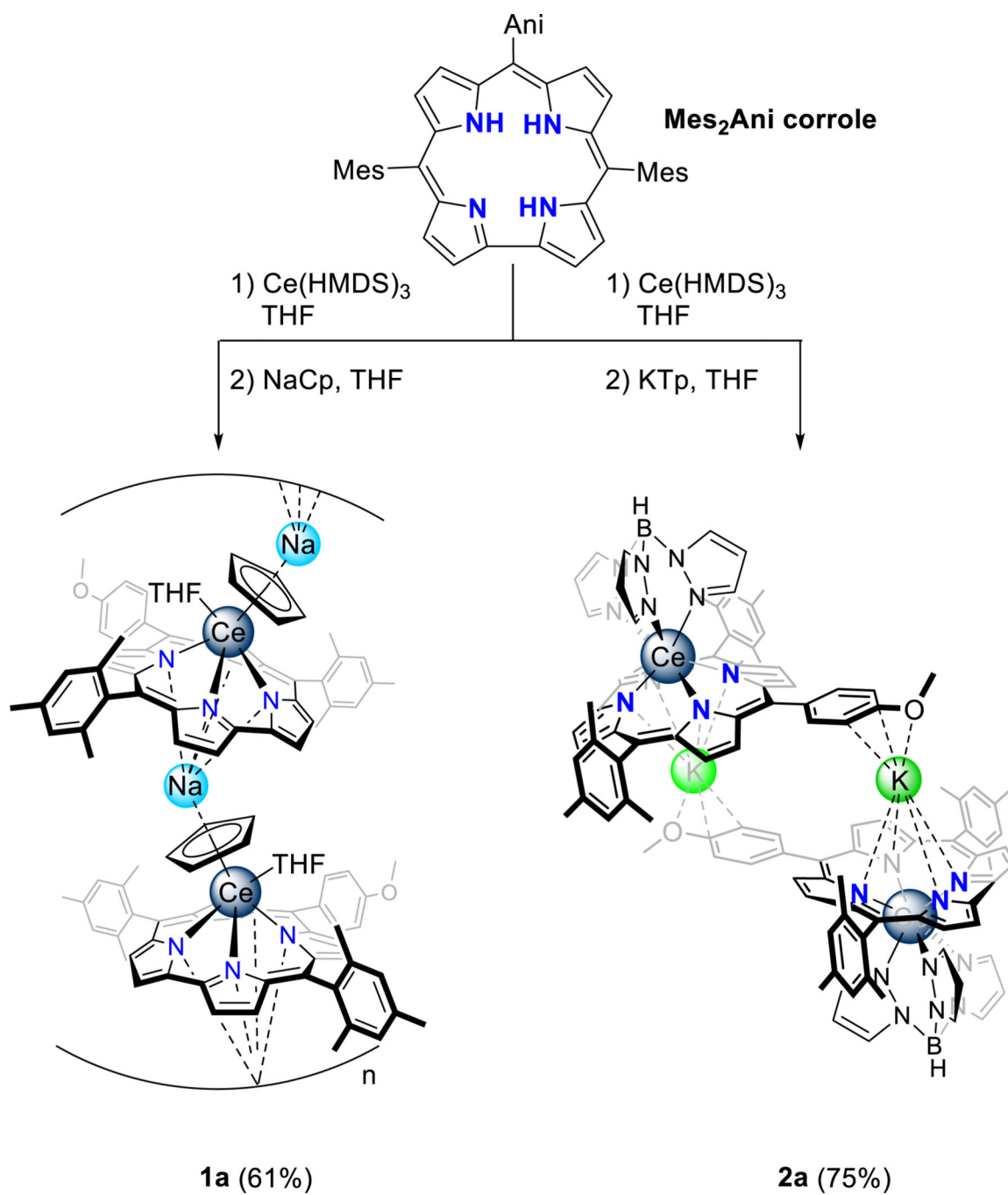
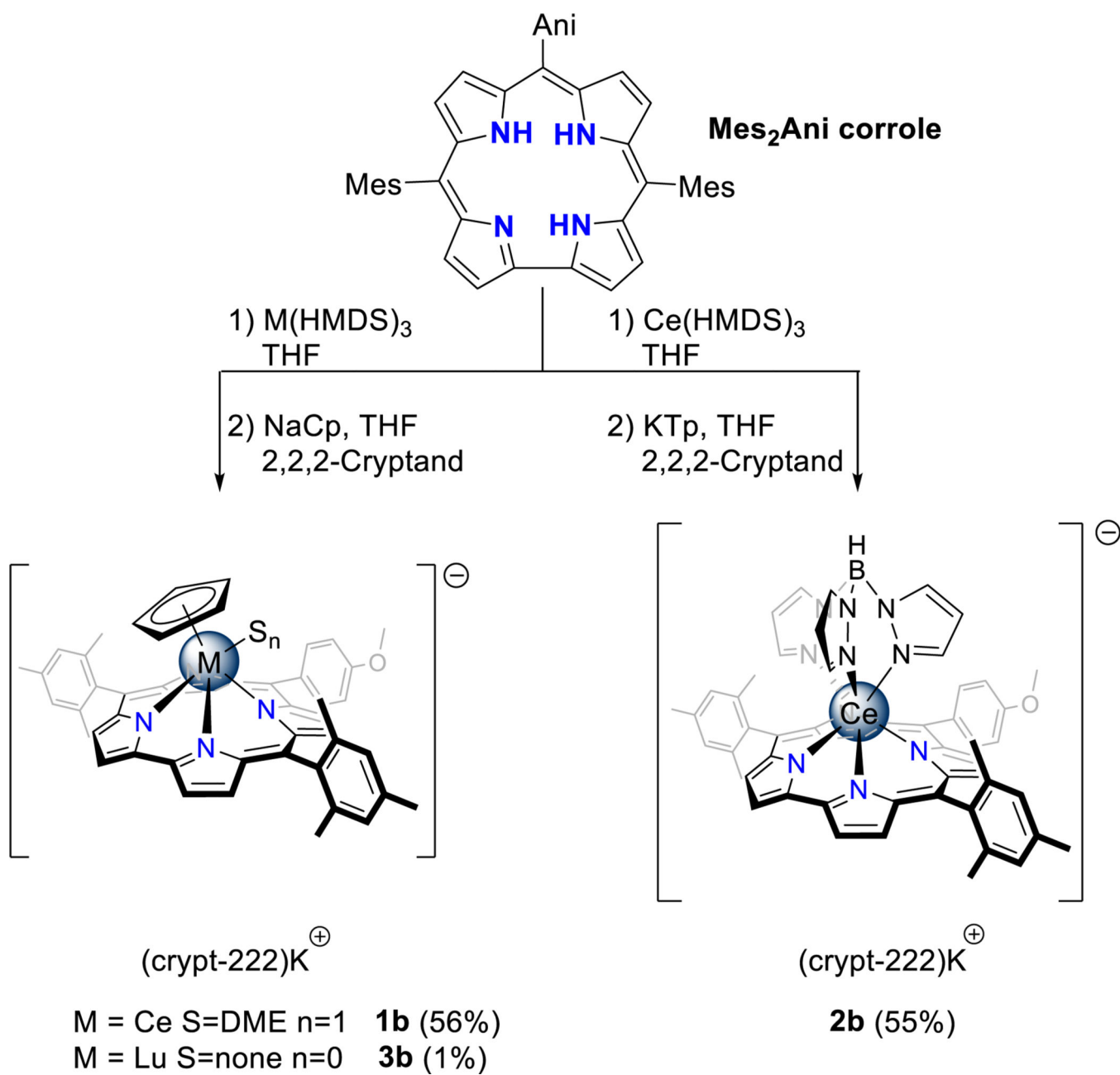


Figure 7.
UV/Vis spectra of **2a** and **2b** recorded in THF.



Scheme 1.
Synthesis of complexes **1a** and **2a**



Scheme 2.

Synthesis of complexes **1b**, **2b** and **3b**.